2013

Electromagnetic Characterization of AF455 With DNA-CTMA In Solvent Blends

Jessica Marie Hendricks
Wright State University

ELECTROMAGNETIC CHARACTERIZATION OF AF455 WITH DNA-CTMA IN SOLVENT BLENDS

A thesis submitted in partial fulfillment

of the requirements for the degree of

Master of Science

By

Jessica Marie Hendricks

B.S. in Physics, University of Dayton, 2010

2013

Wright State University

WRIGHT STATE UNIVERSITY

GRADUATE SCHOOL

October 23, 2013

I HEREBY RECOMMEND THAT THE THESIS PREPARED UNDER MY SUPERVISION BY Jessica Marie Hendricks **ENTITLED** Electromagnetic Characterization of AF455 with DNA-CTMA in Solvent Blends **BE ACCEPTED IN PARTIAL FULFILLMENT OF THE REQUIREMENTS FOR THE DEGREE OF** Master of Science.

_____
Gregory Kozlowski, Ph.D.
Thesis Director

_____
Doug Petkie, Ph.D.
Chair, Physics Department
College of Science and Mathematics

Committee on Final Examination

_____
Gregory Kozlowski, Ph.D.

_____
Doug Petkie, Ph.D.

_____
Angela L. Campbell, Ph.D.

_____
David Stewart, Ph.D.

_____
R. William Ayres, Ph.D.
Interim Dean, Graduate School

ABSTRACT

Hendricks, Jessica Marie, M.S. Department of Physics, Wright State University, 2013.
Electromagnetic Characterization of AF455 with DNA-CTMA in Solvent Blends.

This work studies the electromagnetic properties of AF455, a two photon dye, DNA bound with cetyltrimethyl ammonium (CTMA), in liquid solvent blends for use in thin film optical filters. The liquid properties of the materials are believed to be transferred to the films. The solvent blends used are ratios of toluene (T) and dimethyl sulfoxide (DMSO). The complex permittivity and permeability of the samples are measured using the short open coaxial line technique in the frequency range of 1.0×10^7 Hz to 2.0×10^9 Hz. In this frequency range, AF455 does not act as a two photon absorber. The results show there is an interaction between AF455 and DNA-CTMA that increases the real permittivity for two solvent blends (50-50, and 60-40, T-DMSO). There is also a clear conformation change in the samples with the solvents and DNA-CTMA only that is observed in the real permittivity. In the 70-30 blend, the conformation of the DNA-CTMA is a clear helix. In the samples with less toluene the conformation of the DNA-CTMA is a coil structure. The imaginary permittivity increases with the addition DNA-CTMA. The real and imaginary permeability are constant across all samples.

TABLE OF CONTENTS

TABLE OF CONTENTS (Cont'd)

LIST OF FIGURES

LIST OF FIGURES (Cont'd)

LIST OF TABLES

ACKNOWLEGEMENTS

I would like to thank my family and friends for supporting me through this whole graduate school process. I know it was as difficult for my parents and my sister to help me through this whole process. I thank Jasmynn for all our weekly evenings reducing my stress. I thank Angela Campo who went through this process recently and was able to tell me what I might not be expecting to see that was important. I thank Adam Davis for the discussions we had.

At Wright-Patterson Air Force Base, I would like to thank Dr. Angela Campbell for funding this research, guiding me, and agreeing to be on my committee. I want to thank Dr. David Stewart for being patient with me while I tried to understand the chemistry and for being on my committee. I thank Dr. Tom Cooper for assisting me and keeping my project after Dr. Campbell left. Thanks to Dr. Doug Krein for his assistance in the lab and looking over my thesis. I thank Hadil Issa for her conversations and assistance.

At the University of Cincinnati, I thank Dr. Richard Kleismit for his help in collecting and processing the data. I thank Dr. David Mast answering my questions and allowing me access to his lab.

At Wright State University, I give lots of thanks for all the assistance from Dr. Gregory Kozlowski who assisted me in finding research at WPAFB, his time and patience in helping through the research and thesis process. I have learned so much from Dr. Kozlowski and it has been a pleasure working with him. I want to thank Dr. Petkie for agreeing to be on my committee and helping me finish my degree in a timely way.

DEDICATION

I dedicate this thesis to Mr. Art Ross without whom I would not be where I am today. He guided me through physics allowing me to fall in love with the subject and profession. He is greatly missed.

1.0 INTRODUCTION

The two photon absorption (TPA) molecule, AF455, can be used in thin films as an optical filter[1]. A TPA molecule absorbs two photons of lower energy instead of a single higher energy photon (see Figure 1).

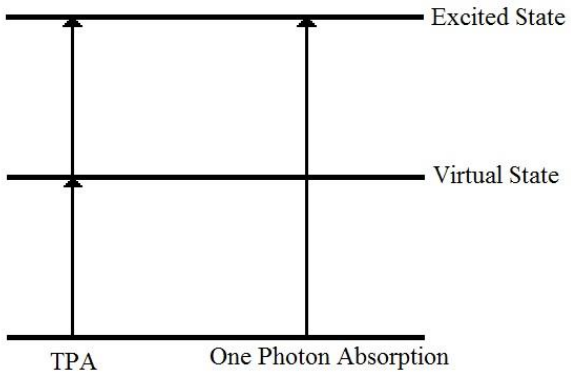

Figure 1. Two Photon Schematic

The energy of the photon in the TPA process is half of the value of the single photon which reduces the exposure to higher energy, more damaging photons. The peak of TPA is 419 nm in toluene and dimethyl sulfoxide blends for AF455. Previous research has shown there is an increase in the absorption of two photons when AF455 binds with DNA-CTMA (cetyltrimethyl ammonium)[2].

DNA is used to create thin films and biosensors[3]. The optical/electromagnetic properties of DNA-CTMA can vary with its conformation which is the shape of the molecule. Two common conformations of DNA-CTMA are a coil or a helix. The permittivity of the DNA-CTMA varies depending on the conformation and how it is processed[4,5,6,20]. The permittivity of

DNA can be as high as 80 for a helix[7] or as low as 7[8]. The permittivity for a coil is automatically lower than the permittivity for a helix. Figure 2 shows some possible conformations of DNA[9].

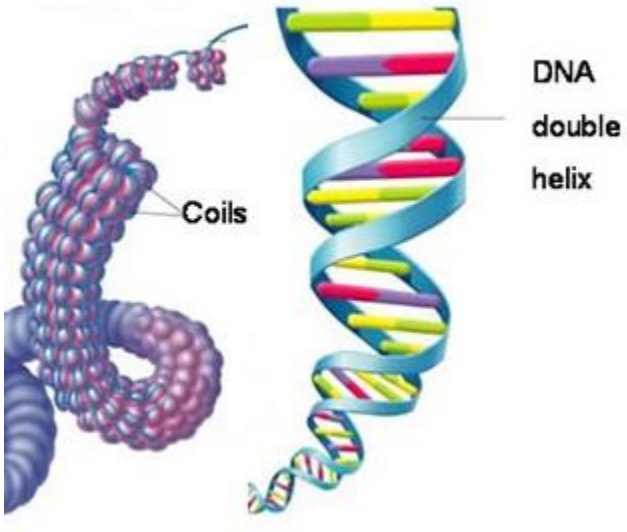

Figure 2. DNA Conformations (Coil and Helix)[7]

DNA readily dissolves in water, but does not dissolve in other organic solvents. To make thin films with DNA, it must be bound to CTMA[4,10]. The DNA-CTMA can then be dissolved in dimethyl sulfoxide (DMSO). AF455 does not dissolve in DMSO, to compensate for this, AF455 must be dissolved in toluene. There is a possible interaction between the two solvents, toluene and DMSO, that may affect the permittivity[11]. This will be further explored in Section 4.1. The fluid consisting of all these materials can be spin-coated or deposited by matrix assisted pulsed laser evaporation (MAPLE) to produce thin films[12]. It is believed the properties of the liquid are transferable to the films[5].

This work investigates the electromagnetic characteristics of AF455 with DNA-CTMA in several ratios of toluene to DMSO at 1.0×10^7 Hz to 2.0×10^9 Hz. AF455 does not behave as a TPA in this range, but single photon absorption can still occur. This work will look into whether

permittivity will increase in single photon absorption when AF455 and DNA-CTMA bind. Another interesting aspect this work will investigate is how the conformation of DNA-CTMA will affect the permittivity. Since the DNA molecule is very polar in its helix conformation, the permittivity should increase when it is in this conformation. This will also give an additional indicator to the conformation of polar molecules in addition to circular dichroism. Chapter two discusses the theoretical background of permittivity and permeability and their relationship to optical properties. Chapter three describes the materials and measurement techniques. Chapter four presents the results and discusses the meaning of those results. The final chapter, Chapter five, summarizes the results and offers areas of further research.

2.0 THEORETICAL BACKGROUND

This chapter will look at the background information in the following order: permittivity, permeability, relationship to optical properties, and finally, TPA.

2.1 Permittivity

The permittivity is a measure of how easily a material polarizes in response to an electric field. The dipole moment determines the material's polarization. The polarization is the net dipole moment per unit volume. A material can be polarized by two different mechanisms. The first is when an applied external electric field induces dipole moments. The second scenario involves an already polar material, which has a permanent dipole moment[13].

The polarization relates to the permittivity in the following manner. The polarization, $\vec{P}$, is proportional to the electric field, $\vec{E}$, by

$$\vec{P} = \varepsilon_0 \chi_e \vec{E} \tag{1}$$

where ε_0 is the permittivity of free space and χ_e is the relative electric susceptibility. A material that follows Equation 1 is a linear dielectric and describes linear optical properties. The displacement field, $\vec{D}$, describes the overall electric field in the material. It is defined by Equation 2.

$$\vec{D} = \varepsilon_0 \vec{E} + \vec{P} \tag{2}$$

Further simplifying of Equation 2 leads to:

$$\vec{D} = \varepsilon_0 \vec{E} + \varepsilon_0 \chi_e \vec{E} \tag{3}$$

$$\vec{D} = \varepsilon_0 (1 + \chi_e) \vec{E} \tag{4}$$

$$\vec{D} = \varepsilon_0 \varepsilon_r \vec{E} \tag{5}$$

$$\varepsilon_r \equiv (1 + \chi_e) \tag{6}$$

where ε_r relative permittivity. In general, ε_r is a complex number.

$$\varepsilon_r = \varepsilon' + i\varepsilon'' \tag{7}$$

The real part of the permittivity, ε', represents how much energy the material is able to store and the imaginary part, ε", represents how dissipative the material is. The loss tangent, Equation 8, compares the amount of energy lost to the amount of energy stored. Generally, one does not want a very lossy material.

$$\frac{1}{Q_\varepsilon} = Tan\delta = \frac{\varepsilon''}{\varepsilon'} \tag{8}$$

The reciprocal of the loss tangent is the quality factor, Q_ε, which describes how much energy the material stores. Figure 3 shows the frequency dependence of relative permittivity between10^3 and 10^{17} Hz[14].

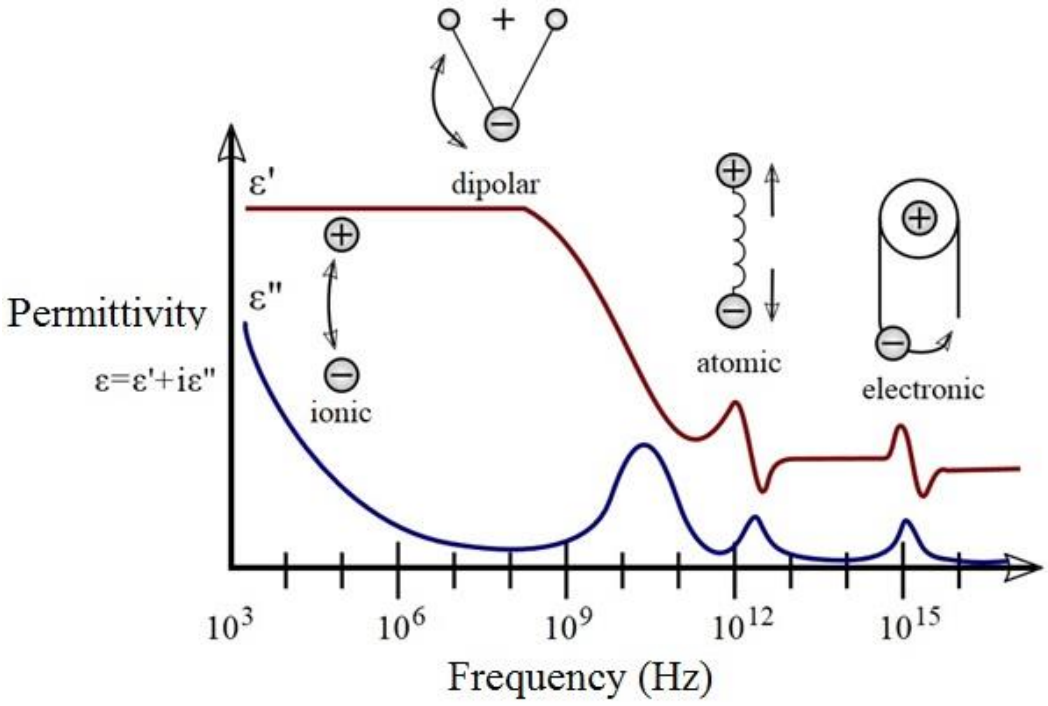

Figure 3. Relationship Between ε' and ε'' with Respect to Frequency[14]

In the region of interest in this study, dipolar interactions will be the dominant mechanism responsible for permittivity. Other mechanisms, ionic, atomic, and electronic, are responsible for the permittivity outside the range of interest. When an electric field is applied, the distance between charges remains constant for a material with a permanent dipole moment. The molecules will attempt to reorient themselves in response to the external electric field. The overall permittivity is the addition of all the individual dipole moments of the material. If the material does not have a permanent dipole moment, an electric field can induce one. This induced dipole moment then contributes to the permittivity. This is what is meant by the dipolar interactions in Figure 3.

2.2 Permeability

Permeability is similar to permittivity, but describes the response of the material with respect to magnetic fields[15]. The magnetization of a material is defined by $\vec{M}$, which is the magnetic dipole moment per unit volume. The auxiliary field, $\vec{H}$, is used to find the relationship between the magnetization and the permeability. The external magnetic field, $\vec{B}$, is produced by current. There are two different pieces of the current: the free current, $\vec{J}_{free}$, and the bound current, $\vec{J}_{bound}$. The free current induces the magnetic field due to the movement of charge. The bound current is due to the magnetization of the material, the aligned magnetic dipoles. Using Ampere's Law,

$$\vec{\nabla} \times \vec{B} = \mu_0 \vec{J} + \mu_0 \varepsilon_0 \frac{\partial \vec{E}}{\partial t} \tag{9}$$

with the definition of the current density,

$$\vec{J} = \vec{J}_{free} + \vec{J}_{bound} \tag{10}$$

the relationship between the auxiliary field, magnetic field, and magnetization can be found. At low frequencies, the change of the electric field is small, therefore, the second term on the right side of Equation 9 is neglected.

$$\vec{\nabla} \times \vec{B} = \mu_0 \vec{J} = \mu_0 (\vec{J}_{free} + \vec{J}_{bound}) \tag{11}$$

$$\vec{\nabla} \times \vec{B} = \mu_0 (\vec{J}_{free} + (\vec{\nabla} \times \vec{M})) \tag{12}$$

where μ_0 is the permeability of free space and the bound current in the material is defined as

$$\vec{J}_{bound} = \vec{\nabla} \times \vec{M} \tag{13}$$

Simplifying Equation 12 leads to

$$\nabla \times \left(\frac{1}{\mu_0}\vec{B} - \vec{M}\right) = \nabla \times \vec{H} = \vec{J}_{free} \tag{14}$$

$$\vec{H} = \frac{1}{\mu_0}\vec{B} - \vec{M} \tag{15}$$

Now, with the definition of the auxiliary field, the relationship between it and the magnetization can be given as follows

$$\vec{M} = \chi_m \vec{H} \tag{16}$$

where χ_m is the magnetic susceptibility. Like the electric materials that obey Equation 1, materials that obey Equation 16 are also linear materials. Finding the relative permeability is similar to that of the relative permittivity.

$$\vec{B} = \mu_0(\vec{H} + \vec{M}) = \mu_0(1 + \chi_m)\vec{H} = \mu_0\mu_r\vec{H} \tag{17}$$

$$\mu_r \equiv (1 + \chi_m) \tag{18}$$

If this relative permeability value is a scalar value, then the material is isotropic and behaves in the same manner from any direction. If the value is a tensor, it is anisotropic. In this work, only linear materials will be discussed.

There are three possible values for the relative permeability: $\mu_r < 1$, $\mu_r = 1$, $\mu_r > 1$. The first case is where the material is diamagnetic. The second case is in a vacuum. The third case is where the material is paramagnetic or ferromagnetic. For both diamagnetic and paramagnetic cases, the material only displays the magnetism under an externally applied magnetic field. For a diamagnetic material the dipoles align themselves antiparallel to the external field. Paramagnetic dipoles align themselves parallel to the field. When the field is removed, the dipoles in both types of material become randomly oriented.

The relative permeability is also a complex number.

$$\mu_r = \mu' + i\mu'' \tag{19}$$

The real part of the permeability, μ', is the storage term and the imaginary part, μ", is the loss term, just like in permittivity. Usually, the effects of permeability at low frequencies are quite small. There is also a quality factor akin to the permittivity quality factor (Equation 20).

$$\frac{1}{Q_\mu} = Tan\delta = \frac{\mu''}{\mu'} \tag{20}$$

2.3 Optical Properties

This section will relate the permittivity and permeability to the optical properties of a material[13]. Beginning with Maxwell's equations (Equations 21-24) the wave equation for electromagnetism can be found.

$$\vec{\nabla} \cdot \vec{D} = \rho \tag{21}$$

$$\vec{\nabla} \cdot \vec{B} = 0 \tag{22}$$

$$\vec{\nabla} \times \vec{E} = -\frac{\partial \vec{B}}{\partial t} \tag{23}$$

$$\vec{\nabla} \times \vec{H} = \vec{J}_{free} + \frac{\partial \vec{D}}{\partial t} \tag{24}$$

Using the equations for the displacement field, Equation 5, and the auxiliary field, Equation 17, and setting the free current and electric charge density equal to zero:

$$\nabla \times \vec{E} = -\mu_0 \mu_r \frac{\partial \vec{H}}{\partial t} \tag{25}$$

$$\nabla \times \vec{H} = -\varepsilon_0 \varepsilon_r \frac{\partial \vec{E}}{\partial t} \tag{26}$$

by taking the curl of Equation 25 and using Equation 26, the electromagnetic wave equation is obtained.

$$\nabla^2 \vec{E} = \varepsilon_0 \varepsilon_r \mu_0 \mu_r \frac{\partial^2 \vec{E}}{\partial t^2} \tag{27}$$

where the wave velocity, v, is

$$\frac{1}{v^2} = \varepsilon_0 \varepsilon_r \mu_0 \mu_r \tag{28}$$

For an electromagnetic wave in vacuum, Equation 28 becomes:

$$\frac{1}{c^2} = \varepsilon_0 \mu_0 \tag{29}$$

$$c = \frac{1}{\sqrt{\varepsilon_0 \mu_0}} \tag{30}$$

From Equations 28-30 it is easy to see that the velocity of an electromagnetic wave through a medium is

$$v = \frac{c}{\sqrt{\varepsilon_r \mu_r}} \tag{31}$$

To determine the optical properties of a material, a complex value *n* is defined as

$$n = \frac{c}{v} = \sqrt{\varepsilon_r \mu_r} \tag{32}$$

The real part, n', is the velocity of an electromagnetic wave through a material and is the index of refraction. The imaginary part, n'', is the extinction coefficient.

$$n = n' + in'' = \sqrt{(\varepsilon' + i\varepsilon'')(\mu' + i\mu'')} \tag{33}$$

Solving Equation 33 will give the index of refraction and extinction coefficient as a function of permittivity and permeability. The solution is

$$n' = \frac{1}{\sqrt{2}}\Omega \tag{34}$$

$$n'' = \frac{1}{\sqrt{2}}\frac{\varepsilon''\mu' + \varepsilon'\mu''}{\Omega} \tag{35}$$

where Ω is defined by:

$$\Omega \equiv \sqrt{\varepsilon'\mu' - \varepsilon''\mu'' + \sqrt{(\varepsilon'^2 + \varepsilon''^2)(\mu'^2 + \mu''^2)}} \tag{36}$$

To check that Equations 34 and 35 are correct, set $\mu'=1$ and $\mu''=0$ and simplify. The result should give the same result as the derivation when it is assumed in Equation 32 that $\mu_r=1$. Performing the calculation leads to

$$n' = \frac{1}{\sqrt{2}}(\varepsilon' + (\varepsilon'^2 + \varepsilon''^2)^{\frac{1}{2}})^{\frac{1}{2}} \tag{37}$$

$$n'' = \frac{1}{\sqrt{2}}(-\varepsilon' + (\varepsilon'^2 + \varepsilon''^2)^{\frac{1}{2}})^{\frac{1}{2}} \tag{38}$$

Equations 37 and 38 are what is commonly found in textbooks[13]. The index of refraction describes how fast an electromagnetic wave will move through a medium. This is important in optical physics and the details are not discussed here. The extinction coefficient is related to the absorptivity of a material. The relationship will be derived later.

The solution to the electromagnetic wave equation for a wave propagating in the x-direction is

$$E(x,t) = \mathrm{E}_0 e^{i(kx-\omega t)} \tag{39}$$

where k is the wave number, ω is the angular frequency, and E_0 is the amplitude of electric field. For a wave traveling through a medium, the wave number is

$$k = \frac{2\pi n}{\lambda} = \frac{2\pi nf}{c} = \frac{n\omega}{c} \tag{40}$$

Using Equation 40 and expanding *n* into its real and imaginary components, Equation 39 can be written in the following form

$$E(x,t) = \mathrm{E}_0 e^{-n''\omega x/c} e^{i\omega(n'x/c-t)} \tag{41}$$

Finding the intensity, $I = EE^*$, of Equation 41 gives

$$I(x) = E_0^2 e^{-2n''\omega x/c} \tag{42}$$

By direct comparison with Beer's Law for intensity, $I = I_0 e^{-\alpha x}$

$$\alpha = 2n''\omega / c = 4\pi n''/\lambda \tag{43}$$

where λ is the wavelength in vacuum. This gives a measure of how much light will be absorbed by one photon absorption.

2.4 Two Photon Absorption and AF455

The AF455 molecule has the ability to absorb two photons in addition to one photon absorption. TPA is a nonlinear optical process. This process is proportional to the square of intensity instead of being proportional to the intensity as in Beer's Law. The derivation of "Beer's Law" for a TPA is done as follows[16]

$$\frac{dI(x)}{dx} = -BI^2 \tag{44}$$

where B is a constant. Solving the differential equation leads to

$$-\frac{1}{I} = -Bx + G \tag{45}$$

where G is the constant of integration.

$$I = \frac{1}{Bx + G} \tag{46}$$

Applying the boundary conditions ($I(x=0) = I_0$) yields the final result

$$I(x) = \frac{I_0}{I_0 x + 1} \tag{47}$$

However, the AF455 molecule does not always absorb two photons[17]. In the frequency range of this work, the molecule behaves as single photon absorber. The energy range where the molecule acts as a TPA is in the ultraviolet and visible frequency range. This work looks into the properties in the radio frequency range. The energy of the photons in this range is not high enough to see the two photon effects. This allows for the use of the single photon intensity formulas (Equations 42 and 43).

3.0 MATERIALS, METHODS, AND PROCEDURES

This section first discusses the materials used, toluene, DMSO, AF455, and DNA-CTMA. Then it will discuss the method used to make the liquid samples. Finally, a description of the short open coaxial line technique and circular dichroism concludes the chapter.

3.1 Materials

The materials used are toluene, DMSO, AF455, and DNA-CTMA. The details of these substances are described in the following four sections.

3.1.1 Toluene

Toluene is a common organic solvent. It is used in this work for the purpose of dissolving the TPA molecule. Toluene has a very low relative permittivity, 2.38 at 23°C, and has a small dipole moment, 0.375 C·m. Common properties of toluene are summarized in Table 1.[18]

Table 1. Properties of Toluene[18]

Toluene Physical Properties			
Synonym	Methylbenzene	**Beilstein Registry**	635760
Molecular Formula	$C_6H_5CH_3$	**EG/EC Number**	2036259
Molecular Weight	92.14	**MDL Number**	MFCD00008512
CAS Number	108-88-3	**Vapor Pressure**	22 mm Hg (20°C)
Density	0. 865 g/mL at 25ºC	**Dielectric Constant**	2.38 at 23ºC
Boiling Point	110-111ºC	**Dipole Moment**	0.375
Melting Point	-93ºC	**UV cutoff**	286 nm
Flash Point	4.4ºC	**Refractive Index**	1.496 at 20ºC
Viscosity	0.560 at 25ºC	**Vapor Density**	3.2 (vs. air)
RIDADR	UN 1294 3/PG 2	**Risk Statements**	11-38-48/20-63-65-67
Hazard Codes	F,Xn	**Safety Statements**	36/37-46-62

3.1.2 Dimethyl Sulfoxide (DMSO)

Dimethyl sulfoxide, DMSO, is a solvent with many medical, biological, and chemical applications. It is a very polar molecule and has the highest relative permittivity (47.24 at 20°C) of all the substances used in this study. DMSO is used because it dissolves the DNA-CTMA easily. Table 2 displays the properties of DMSO[18].

Table 2. Properties of DMSO[18]

Dimethyl Sulfoxide Physical Property			
Synonym	Methyl sulfoxide	**Beilstein Registry**	506008
Molecular Formula	$(CH_3)_2SO$	**EG/EC Number**	2006643
Molecular Weight	78.13	**MDL Number**	MFCD00002089
CAS Number	67-68-5	**Vapor Pressure**	0.42 mm Hg (20°C)
Density	1.100 g/mL at 25ºC	**Dielectric Constant**	47.24 at 20ºC
Boiling Point	189ºC	**Dipole Moment**	3.960
Melting Point	16-19 ºC	**UV cutoff**	265 nm
Flash Point	85.0°C	**Refractive Index**	1.479 at 20ºC
Viscosity	1.990 at 25°C	**Vapor Density**	2.7 (vs. air)

3.1.3 AF455

AF455 is an organic dye that can absorb two photons in the UV-Vis range. Figure 4 shows the structure of AF455[17]

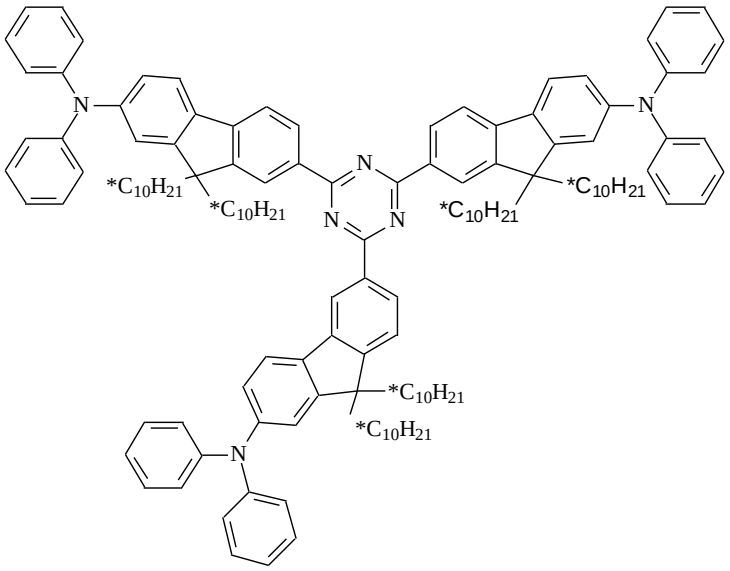

Figure 4. Structure of AF455

Table 3 shows some of the known properties of AF455[17].

Table 3. Properties of AF455

Formula	$C_{138}H_{174}N_6$
Molecular Weight (g/mol)	1916.94
Max Absorption λ for TPA in toluene (nm)	419
Extinction Coefficient at 419 nm ($cm^{-1}\cdot mol^{-1}$)	63.01/cm·mol
Index of Refraction, n	1.64
Net Dipole Moment	0

3.1.4 DNA-CTMA

Salmon DNA is used in this work. This must be bound to cetyltrimethyl ammonium (CTMA) to enable it to dissolve in organic solvents such as DMSO[6,10]. It has been discovered that binding DNA-CTMA with the AF455 increases the absorbance of AF455[2,5]. DNA is a polar molecule, however, the conformation of the molecule will affect this. The environment determines the conformation, it can be in a coil or a helix form. If it is in a coil, the polarity will not be as prominent as it would be if the DNA is in a helix form.

3.2 Preparation of Samples

This section describes the preparation of all the samples: toluene and DMSO blends, AF455 plus the solvent blends, DNA-CTMA plus the solvent blends, and AF455 plus DNA-CTMA plus the solvent blends.

3.2.1 Toluene/DMSO Ratios

The first set of samples does not include either the AF455 dye or the DNA-CTMA. Each sample had a total volume of 10 mL, the volume of toluene or DMSO was pipetted from a bottle of the solvent according to Table 4.

Table 4. Toluene and DMSO Sample Ratios

Sample	Toluene (%)	DMSO (%)
1	70	30
2	60	40
3	50	50
4	40	60
5	30	70

3.2.2 Toluene/DMSO Ratios with AF455

The second set of samples included the AF455 dye. The AF455 stock was made using the following procedure. The powder was weighed on a Sartorius Research balance to 2.54 mg. This was then transferred to a 25 mL flask and diluted with toluene. The AF455 dissolved easily into the toluene. The concentration of the stock solution was 0.10160 mg/mL. Then 0.20 mL of this stock was pipetted into the large vials. Toluene was then pipetted into the vials in an appropriate amount to make the correct percentage of toluene to DMSO. DMSO was pipetted in last, making the total volume of each vial 10 mL. This procedure allowed each sample to have the same AF455 concentration, which allows for direct comparison of their photophysical properties. Tables 5 and 6 display the volume and ratios for the AF455 samples.

Table 5. Volume for AF455 Solutions

Sample by % Tol	AF455 Stock (mL)	Toluene (mL)	DMSO (mL)
30	0.2	2.8	7.0
40	0.2	3.8	6.0
50	0.2	4.8	5.0
60	0.2	5.8	4.0
70	0.2	6.8	3.0

Table 6. Toluene and DMSO Sample Ratios with AF455

Sample	Toluene (%)	DMSO (%)	AF455 Concentration (mg/mL)
1	70	30	0.0020
2	60	40	0.0020
3	50	50	0.0020
4	40	60	0.0020
5	30	70	0.0020

3.2.3 Toluene/DMSO Ratios with DNA-CTMA

The third set of samples was made with solid DNA-CTMA. The concentration of each of these five samples needed to be 5.00 mg/mL. This concentration was chosen to match previous data[12]. The DNA-CTMA does not dissolve easily in toluene, so in making the solutions it was best to add only the DMSO initially. After the DNA-CTMA dissolved into the DMSO, the toluene was added. The total volume of liquid was again 10 mL. Table 7 displays the solvent ratios and concentration of DNA-CTMA samples.

Table 7. Toluene and DMSO Sample Ratios with DNA-CTMA

Sample	Toluene (%)	DMSO (%)	DNA-CTMA Concentration (mg/mL)
1	70	30	5.00
2	60	40	5.00
3	50	50	5.00
4	40	60	5.00
5	30	70	5.00

3.2.4 Toluene/DMSO Ratios with DNA-CTMA and AF455

This final set of samples was made with both DNA-CTMA and AF455. The DNA-CTMA was dissolved in DMSO in the same manner as the third set of samples. When adding the toluene, however, the AF455 was added in as well in the same concentration as the second set of samples. The total volume of each sample was 10 mL. The concentrations and ratio of toluene to DMSO is shown in Table 8.

Table 8. Toluene and DMSO Ratios with Both DNA-CTMA and AF455

Sample	Toluene (%)	DMSO (%)	AF455 Concentration (mg/mL)	DNA-CTMA Concentration (mg/mL)
1	70	30	0.0020	5.00
2	60	40	0.0020	5.00
3	50	50	0.0020	5.00
4	40	60	0.0020	5.00
5	30	70	0.0020	5.00

3.2.5 Concentrations of Samples

It is useful to list the concentrations of the samples in a different manner than that above. Table 9 lists the concentrations of the samples by mole fraction, percent mass, and molar concentration.

Table 9. Concentrations of Samples

Sample Set	Sample	Percent by Mass				Molar Concentration (mol/L)			
		Toluene (%)	DMSO (%)	AF455 ($x10^{-4}$ %)	DNA (%)	Toluene	DMSO	AF455 ($x10^{-6}$)	DNA ($x10^{-6}$)
1	0-100	0	100	0	0	0	12.85	0	0
	30-70	27	73	0	0	2.83	9.00	0	0
	40-60	37	63	0	0	3.78	7.71	0	0
	50-50	46	54	0	0	4.72	6.43	0	0
	60-40	57	43	0	0	5.67	5.14	0	0
	70-30	67	33	0	0	6.61	3.86	0	0
	100-0	100	0	0	0	9.44	0	0	0
2	30-70	27	73	2.10	0	2.83	12.85	1.06	0
	40-60	36	63	2.13	0	3.78	9.00	1.06	0
	50-50	46	53	2.16	0	4.72	7.71	1.06	0
	60-40	56	43	2.19	0	5.67	6.43	1.06	0
	70-30	67	33	2.22	0	6.61	5.14	1.06	0
	100-0	99	0	2.32	0	9.44	3.86	1.06	0
3	0-100	0	100	0	0.10	0	12.85	0	5.00
	30-70	27	73	0	0.10	2.83	9.00	0	5.00
	40-60	36	63	0	0.10	3.78	7.71	0	5.00
	50-50	46	53	0	0.11	4.72	6.43	0	5.00
	60-40	56	43	0	0.11	5.67	5.14	0	5.00
	70-30	67	33	0	0.11	6.61	3.86	0	5.00
4	30-70	27	73	2.10	0.10	2.83	9.00	1.06	5.00
	40-60	36	63	2.13	0.10	3.78	7.71	1.06	5.00
	50-50	46	53	2.16	0.11	4.72	6.43	1.06	5.00
	60-40	56	43	2.19	0.11	5.67	5.14	1.06	5.00
	70-30	67	33	2.22	0.11	6.61	3.86	1.06	5.00

3.3 Permittivity and Permeability Measurements

The technique used to measure complex permittivity and complex permeability uses a short and open coaxial line[19]. A signal is sent down the cable and into a sample cell filled with fluid. The reflection coefficient is measured based on the difference between it and the original wave.

The short open coaxial line (SOCL) technique is based on two existing measurement techniques: the short closed coaxial line (SCCL) technique and the open ended coaxial line (OECL) technique. These techniques are not suitable if a large dielectric component of the material is expected. This is because the measurement is not very sensitive if μ is small and ε is large, the SOCL technique does not have this limitation. The SOCL uses two small cavities, one that has an open circuit and the other that has a short circuit. The reflection coefficients, Γ_s (short) and Γ_o (open), are measured and used to determine the complex permittivity and permeability with a high degree of accuracy over a large frequency range.

The system used for these measurements is outlined in red in Figure 5. The Agilent Technologies Network Analyzer sends an outgoing wave though the cable and measures the reflected wave in the small cavity at the end of the coaxial line.

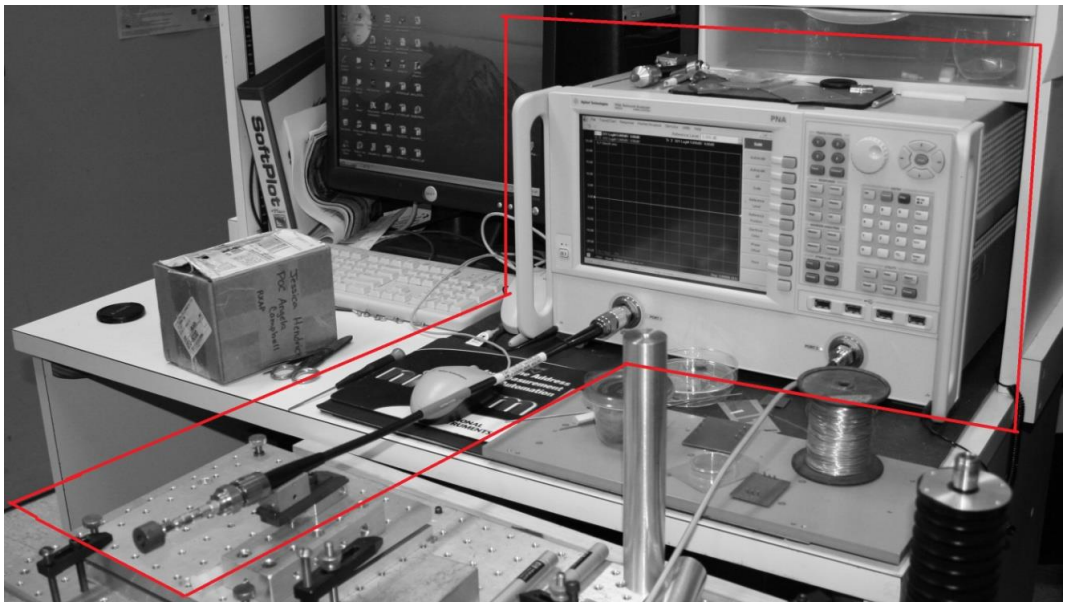

Figure 5. System for SOCL Technique

In Figure 6, A is the top of the probe, B is the short cavity, and C is the open cavity. Figure 7 shows the top view of the cavities. The fluid is injected into the cavity inside of the O-ring. Figures 8 and 9 show the short and open cavities connected to the coaxial line.

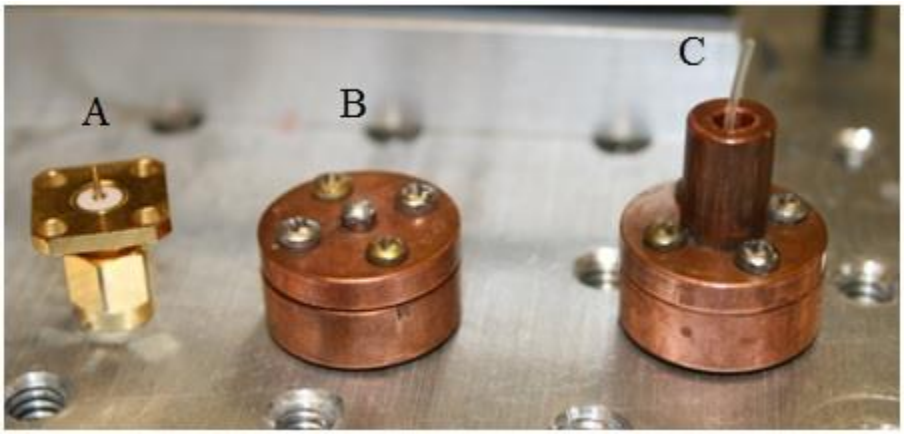

Figure 6. Cavities Used for SOCL Technique (A-Top of Cavity, B-Short Cavity, and C-Open Cavity)

Figure 7. Top View of Cavity

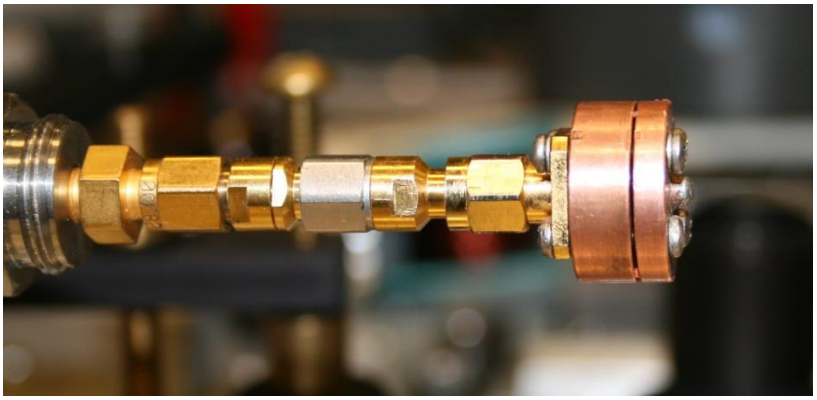

Figure 8. Short Cavity Connected to Probe

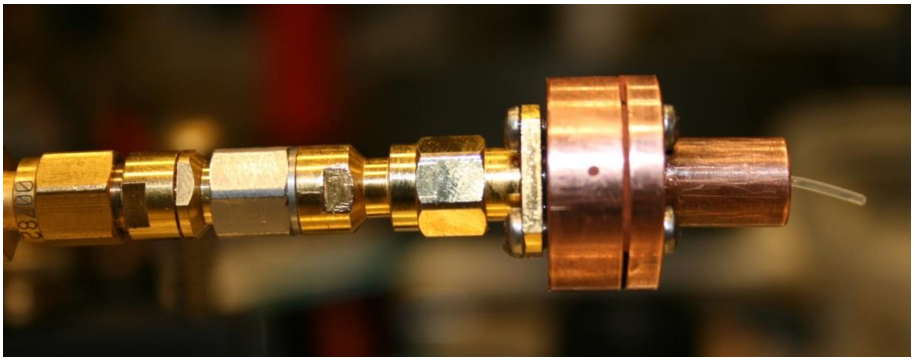

Figure 9. Open Cavity Connected to Probe

The permittivity and permeability are calculated using the reflection coefficients at the input port of a single port coaxial cell of length *L*. The target values are related to the reflection coefficients by the following equations from the SCCL and OECL techniques:

$$i\sqrt{\frac{\mu}{\varepsilon}}Tan(\sqrt{\mu\varepsilon}\beta_0 L)=\frac{1+\Gamma_s}{1-\Gamma_s} \tag{48}$$

$$i\sqrt{\frac{\varepsilon}{\mu}}Tan(\sqrt{\mu\varepsilon}\beta_0 L)=\frac{1-\Gamma_o}{1+\Gamma_o} \tag{49}$$

where $i=\sqrt{-1}$, L is the length of the cell, and $\beta_0$is the free space propagation constant. Rearranging Equations 48 and 49 gives:

$$\frac{\mu}{\varepsilon}=\frac{1+\Gamma_s}{1-\Gamma_s}\frac{1+\Gamma_o}{1-\Gamma_o} \tag{50}$$

$$Tan^2(\sqrt{\mu\varepsilon}\beta_0 L)=-\frac{1+\Gamma_s}{1-\Gamma_s}\frac{1-\Gamma_o}{1+\Gamma_o} \tag{51}$$

From Equations 50 and 51

$$\sqrt{\mu\varepsilon}=\frac{1}{\beta_0 L}ArcTan(\sqrt{-\frac{1+\Gamma_s}{1-\Gamma_s}\frac{1-\Gamma_o}{1+\Gamma_o}}) \tag{52}$$

which leads to

$$\mu=\frac{1}{\beta_0 L}\sqrt{\frac{1+\Gamma_s}{1-\Gamma_s}\frac{1+\Gamma_o}{1-\Gamma_o}}ArcTan(\sqrt{-\frac{1+\Gamma_s}{1-\Gamma_s}\frac{1-\Gamma_o}{1+\Gamma_o}}) \tag{53}$$

$$\varepsilon=\frac{1}{\beta_0 L}\sqrt{\frac{1-\Gamma_s}{1+\Gamma_s}\frac{1-\Gamma_o}{1+\Gamma_o}}ArcTan(\sqrt{-\frac{1+\Gamma_s}{1-\Gamma_s}\frac{1-\Gamma_o}{1+\Gamma_o}}) \tag{54}$$

3.4 Circular Dichroism Measurements

The instrument for the circular dichroism (CD) measurements is the CD Spectrometer J-815. The CD technique uses right and left circularly polarized light to analyze the conformation of asymmetric molecules[20]. Asymmetric biological molecules absorb in one direction more than the other. The CD is the difference between these two absorption values. The resulting light is then elliptically polarized. Figure 10 depicts circularly and linearly polarized light.

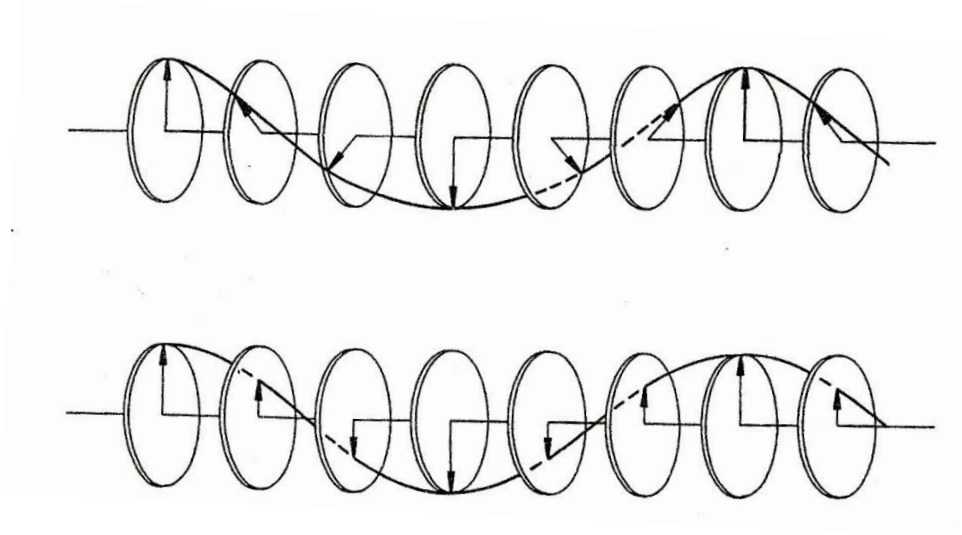

Figure 10. Circularly Polarized Light (Top) and Linearly Polarized Light (Bottom)[20]

Beer's Law is followed for circularly polarized light and the equation for determining the difference in absorption is simply

$$\Delta A = A_{left} - A_{right} = n''_{left} LC - n''_{right} LC = \Delta n'' LC \tag{55}$$

where A is the absorption, L is the sample length, C is the concentration, and n'' is the extinction coefficient. Equation 55 is related to the ellipticity, θ, of the elliptically polarized light. The

tangent of the ellipticity is the ratio between the minor axis and the major axis of the ellipse and due to its small size is equal to θ in radians. From this definition θ is related to ΔA by

$$\theta = 32.98\Delta A \tag{56}$$

where θ is in degrees. The molar ellipticity, $[\theta]$, is given by

$$[\theta] = 3298\Delta n'' \tag{57}$$

where $[\theta]$ has the units deg·cm^2·mol^{-1}. This is the measurement observed on the instrument.

4.0 RESULTS AND DISCUSSION

This chapter discusses the results of the SOCL technique. First, the relative permittivity is discussed followed by the relative permeability.

4.1 Permittivity Measurements

The relative permittivity results are discussed in this section. The real permittivity is discussed first and the imaginary permittivity is discussed second. The results are summarized in the final section.

4.1.1 Real Permittivity

Figure 11 shows the real permittivity vs. frequency for the solvent blends.

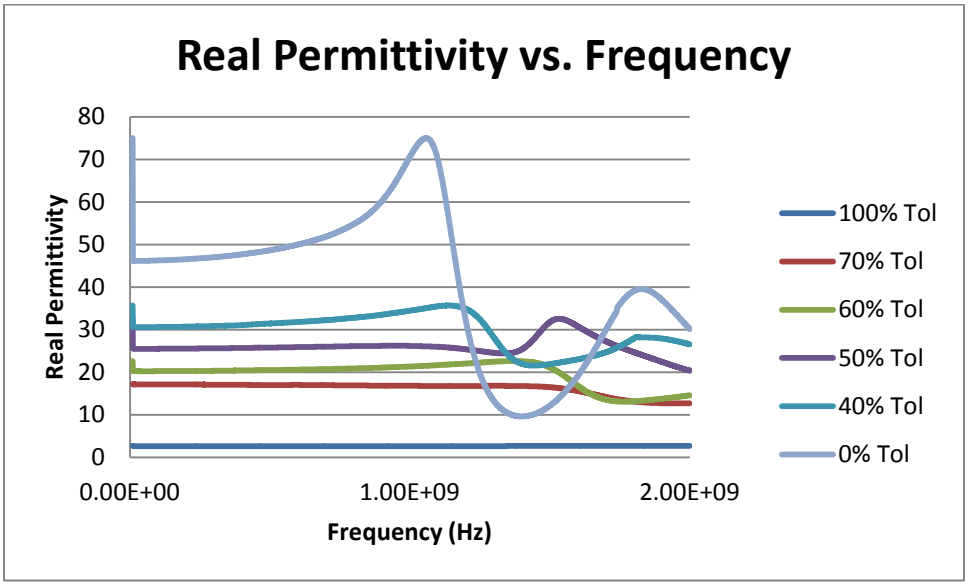

Figure 11. Real Permittivity for Solvent Blends

The data follows the expected path at lower frequencies. At higher frequencies, the resonance of the cavity used in the SOCL technique are evident. This pattern continues through

all of the data hereafter. The known dielectric constant of 100% DMSO is 47.24 and the known dielectric constant of 100% toluene is 2.38. Using these and assuming no interaction between the solvents, the dielectric constant can be predicted using the rule of mixtures, Table 10.

Table 10. Theoretical Dielectric Constants for Mixtures of Toluene and DMSO

Toluene (%)	DMSO (%)	Predicted Real Permittivity	Measured Real Permittivity
0	100	47.24	47.74
30	70	33.78	-
40	60	29.30	30.56
50	50	24.81	25.46
60	40	20.32	20.23
70	30	16.37	17.12
100	0	2.38	2.60

It is clear the theoretical values derived by the theory of mixtures match the values from Table 10. It has been hypothesized that there is an interaction between the two solvents. The conclusions by Thirumaran and Rajeswari[11] are inconsistent with the results here. In their work, they look at aromatic hydrocarbons with DMSO. They hypothesize there to be dipole-dipole and dipole-induced-dipole interactions, but state these interactions are very tiny. The data in Figure 9 and Table 10 indicate there is no interaction between the solvents.

Figure 12 shows the permittivity in the solvents for a frequency of 250 MHz. The nice linear pattern that is expected is evident.

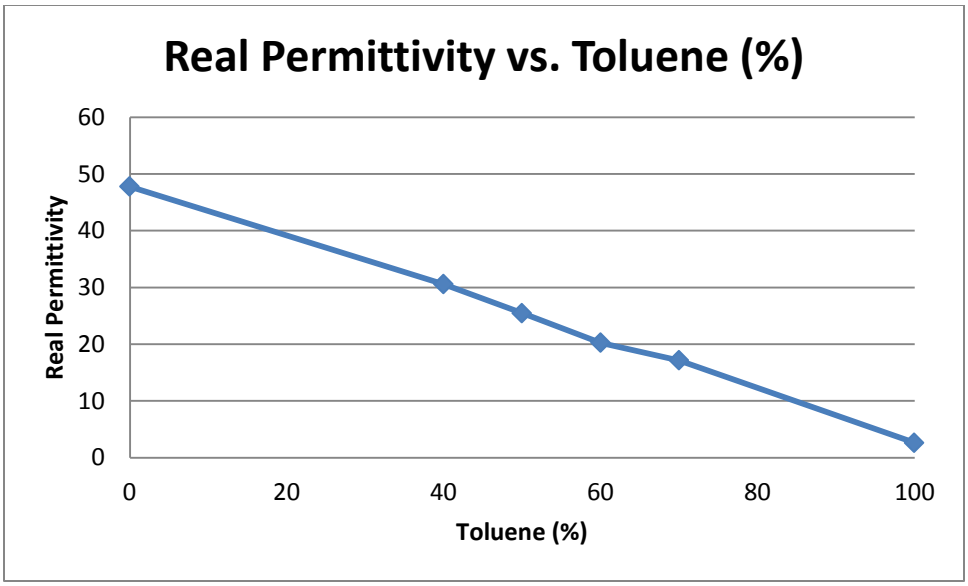

Figure 12. Real Permittivity at 250 MHz

With the addition of AF455, there is a tiny drop of overall permittivity in the solvent blends.

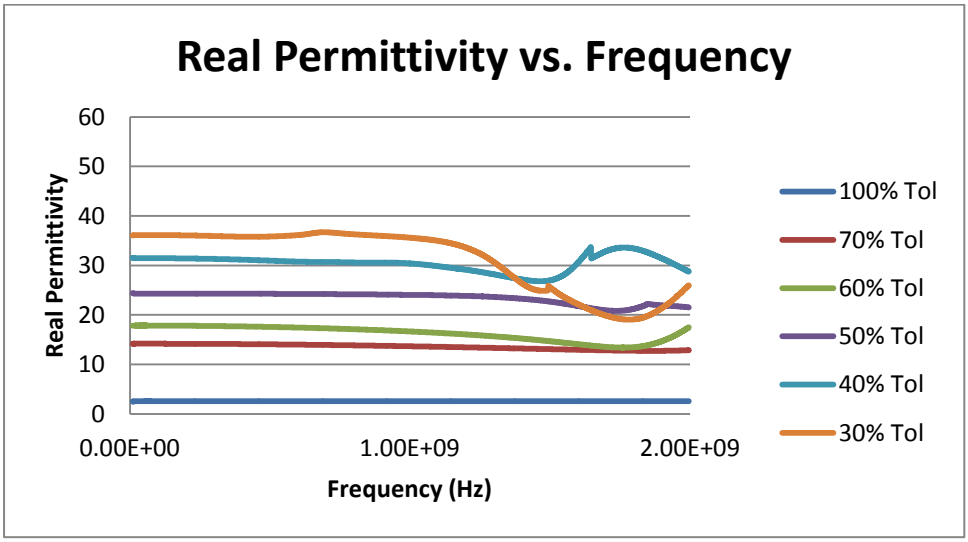

Figure 13. Real Permittivity with AF455

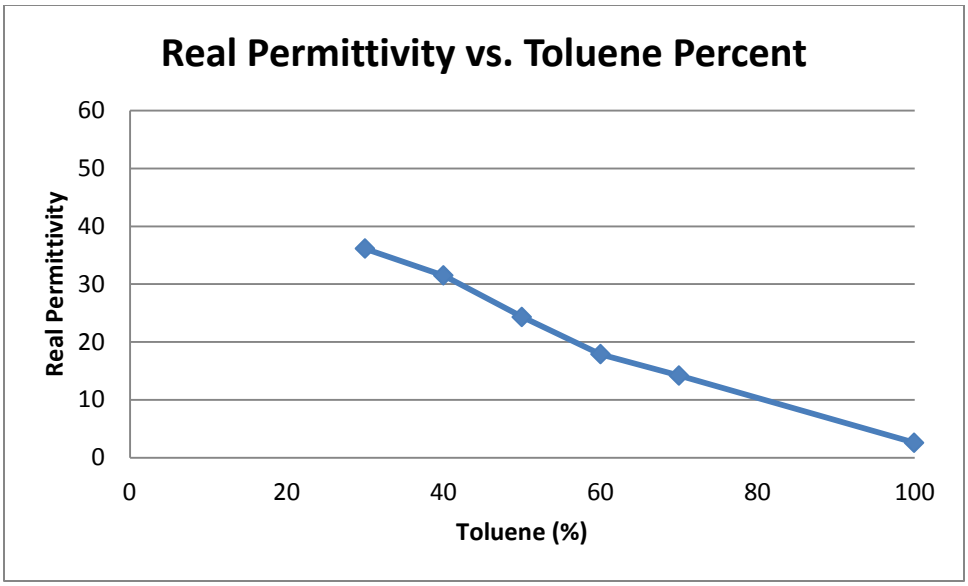

Figure 14. Real Permittivity with AF455 at 250 MHz

The slight overall reduction of real permittivity with AF455 can be attributed to the dipole moment of the "arms" of the AF455 molecule. The structure of AF455 is trigonal planar. It is hypothesized that only one "arm" is oriented in the field with the DMSO. The other two "arms" being oriented in a different direction reduce the overall field.

When DNA-CTMA is added to the solvent mixtures the permittivity remains unchanged for all but one of the mixtures.

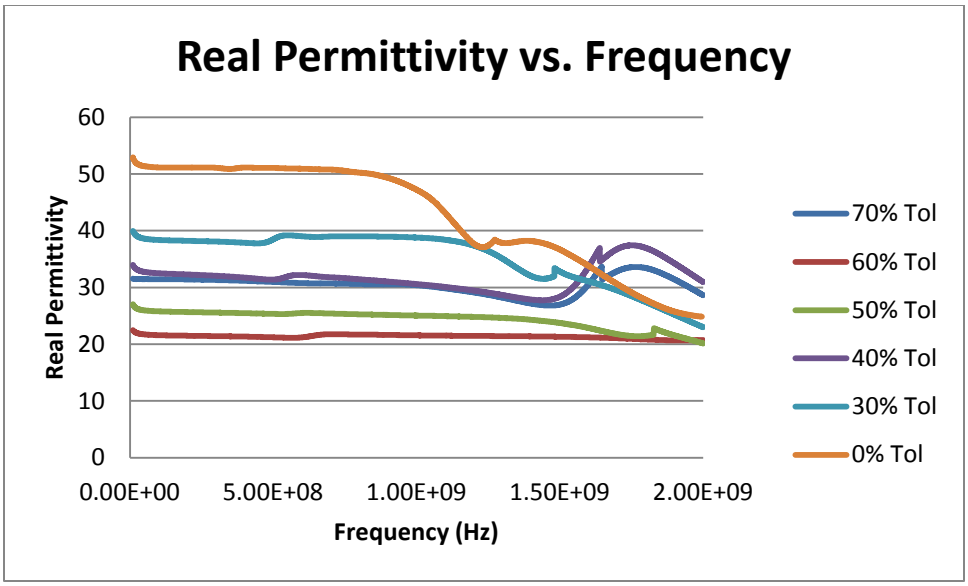

Figure 15. Real Permittivity with DNA-CTMA

The conformation of DNA-CTMA is important in this one case. For most of the mixtures, the DNA-CTMA is in a coil. (See section 4.1.2) This results in no change to the permittivity even though DNA is a polar molecule. In the 70% toluene mixture, however, the DNA-CTMA is in the shape of a helix. This affects the permittivity by increasing it. Figure 16 depicts the data for 250 MHz. The increased polarity of the 70% Toluene solution is easily seen.

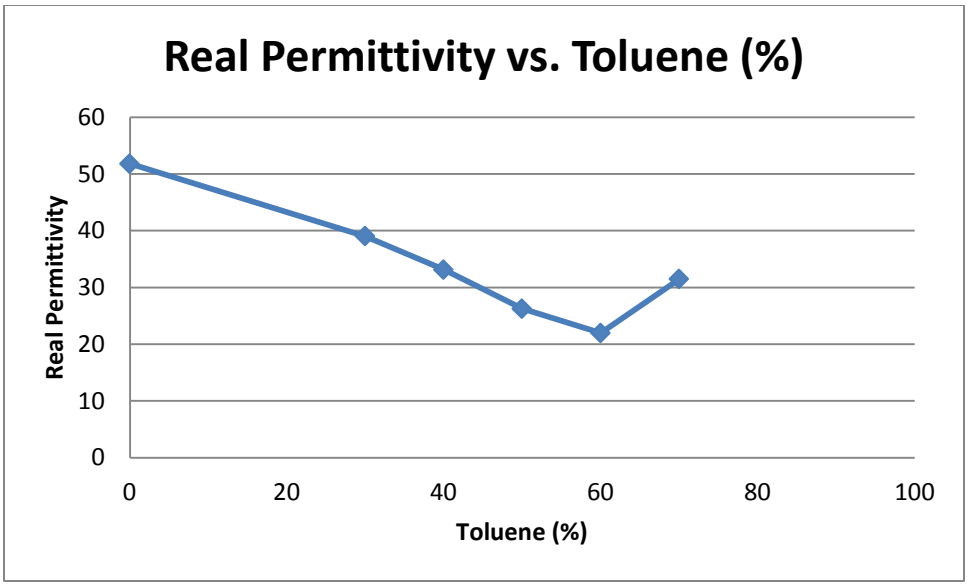

Figure 16. Real Permittivity with DNA-CTMA at 250 MHz

Figure 17 shows real permittivity as a function of frequency for solutions containing both AF455 and DNA-CTMA.

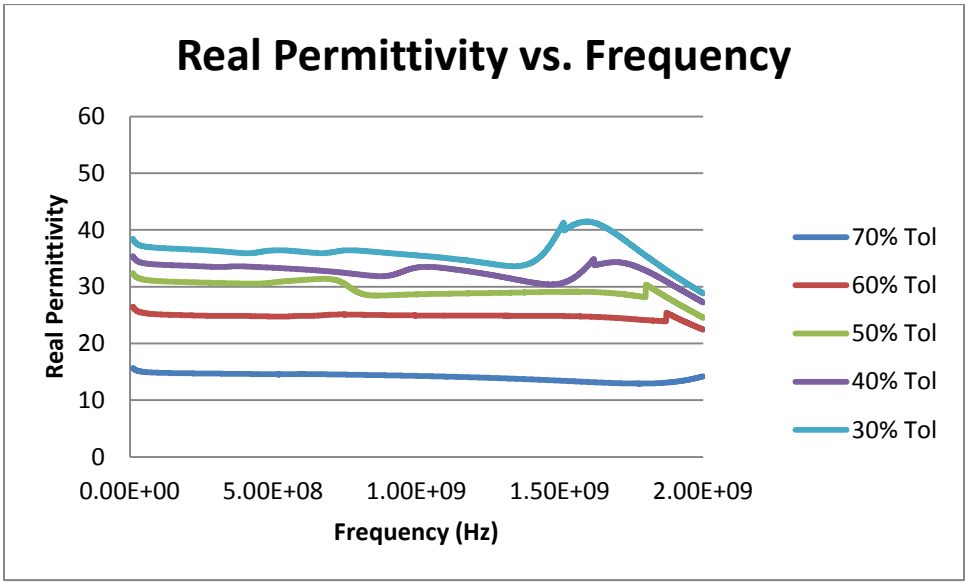

Figure 17. Real Permittivity vs. Frequency for AF455 and DNA-CTMA

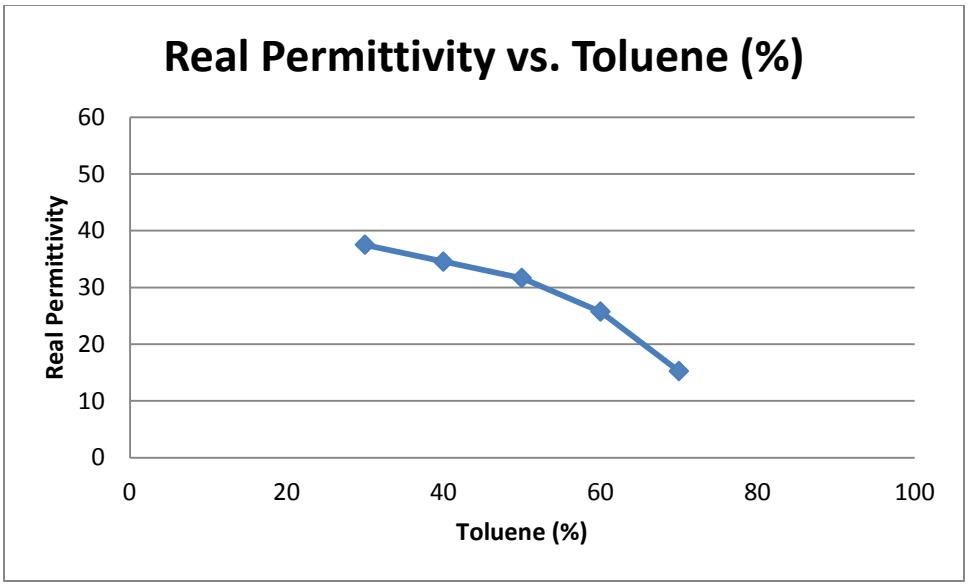

Figure 18. Real Permittivity for AF455 and DNA-CTMA Blends at 250 MHz

For two of the solvent blends (50-50, 60-40), the overall permittivity increases when AF455 and DNA-CTMA are combined. The change could be a result of how the AF455 and DNA-CTMA bind. It is known from previous, parallel studies that when DNA-CTMA binds with AF455 there is an increase in the overall absorbance[2]. In the 70% toluene blend, the conformation change of the DNA-CTMA does not appear. There is an interesting trend in this data that can be modeled. The permittivity, ε_{All}, as a function of the percent of toluene between 30% and 70% is

$$\varepsilon_{All}(x_{Tol}) = -0.0129x_{Tol}^2 + 0.7517x_{Tol} + 26.019 \quad (58)$$

In Figure 19, all of the data is plotted against toluene percent.

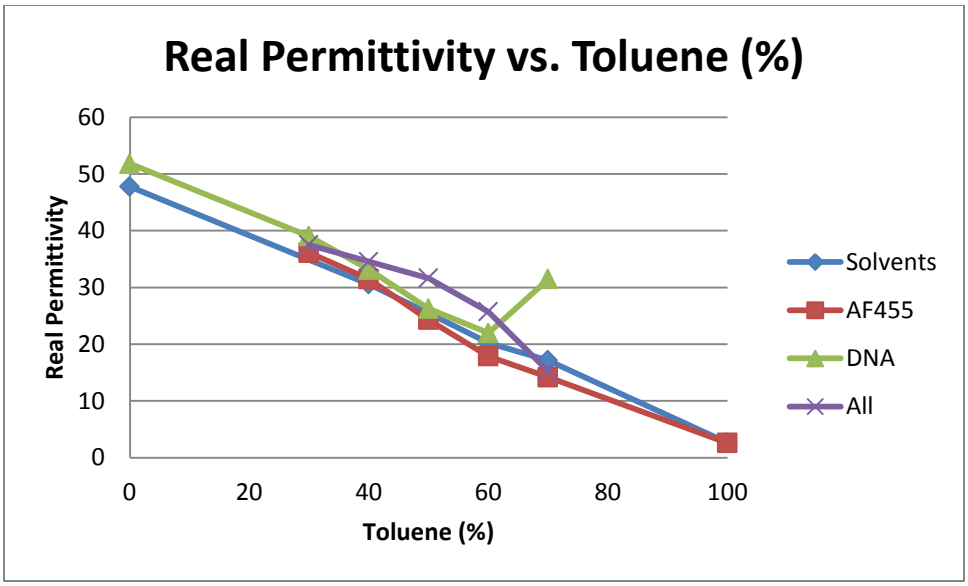

Figure 19. Permittivity vs. Percent Toluene at 250 MHz

The solvent blends and solvents plus AF455 follow a linear pattern. The solvent blends plus DNA-CTMA and all materials do not precisely follow this pattern. In Table 11, the real permittivity values for 250 MHz are listed.

Table 11. Real Permittivity Values at 250 MHz

Percent Toluene	Real Permittivity			
	Solvents	AF455	DNA-CTMA	All
100	2.60	2.57	-	-
70	17.12	14.18	31.47	15.21
60	20.23	17.85	21.96	25.71
50	25.46	24.31	26.25	31.62
40	30.56	31.47	33.12	34.52
30	-	36.12	39.02	37.51
0	47.74	-	51.80	-

4.1.2 Circular Dichroism Measurements

Measurements by circular dichroism provide details on the conformation of DNA. Spin coatings made with the same materials as the permittivity data is used[21]. The use of the spin coatings is necessary because they can be measured directly. If the liquids were used, data would be difficult to obtain because the solvents absorb in the same region of the spectrum as the DNA-CTMA.

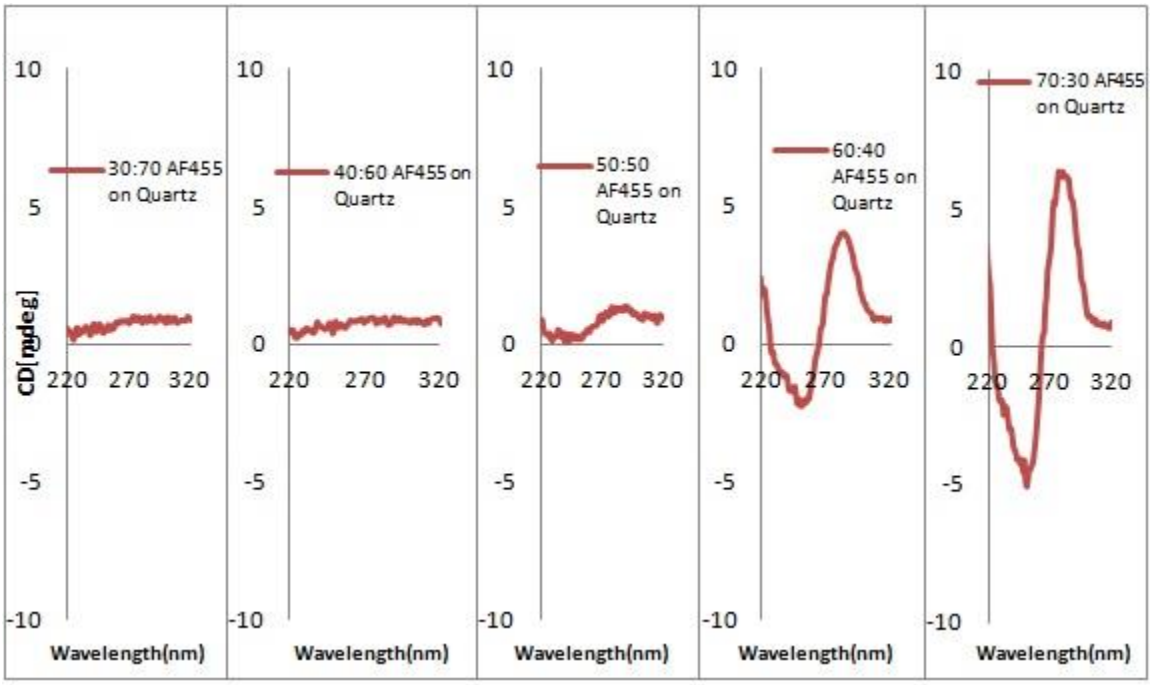

Figure 20. CD Data for Spin Coatings[21]

Figure 20 displays the spin coat data[21]. The graph on the far left displays data for 30% toluene and increases by 10% to 70% toluene displayed to the right. As the toluene percent increases, there is an obvious change in conformation of the DNA in the coating. The DNA for lower toluene is in a coil and in 70% toluene it is clearly a helix. This change is responsible for the increase in permittivity that is seen in Figure 16.

4.1.3 Imaginary Permittivity

The imaginary permittivity should be close to zero[22]. Figures 21 and 22 show imaginary permittivity for the solvent blends.

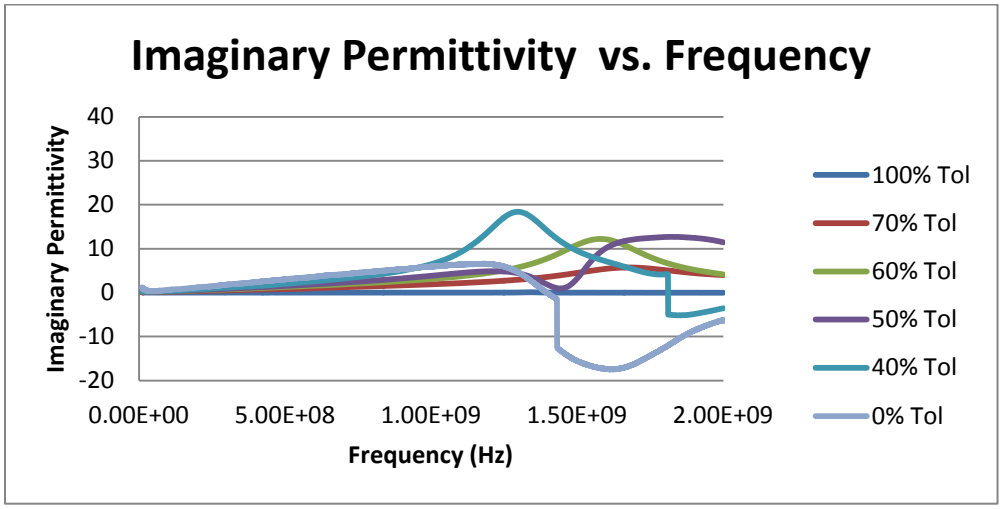

Figure 21. Imaginary Permittivity vs. Frequency for the Solvent Blends

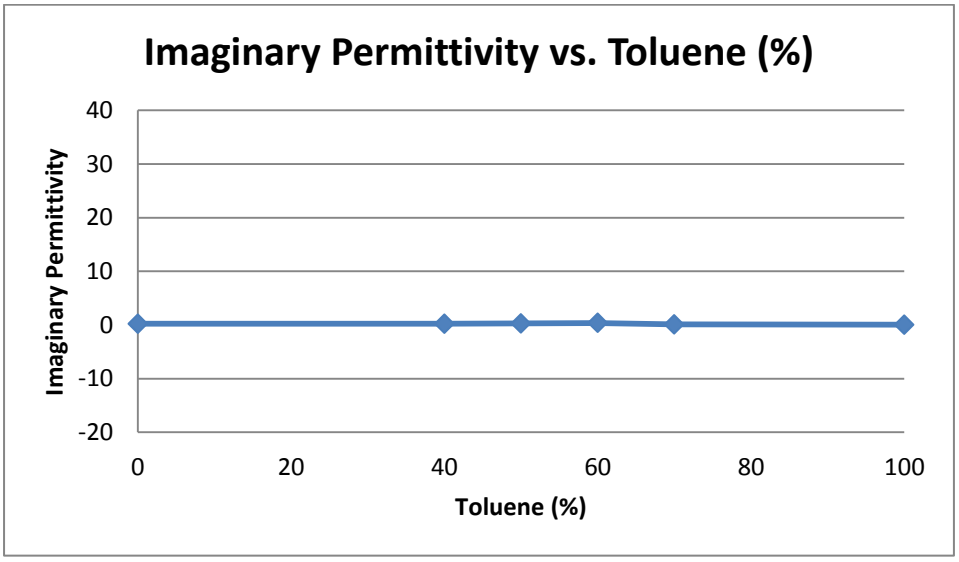

Figure 22. Imaginary Permittivity at 250 MHz

As expected the imaginary permittivity for the solvent blends is roughly zero. Figures 23 and 24 show the results for the addition of AF455.

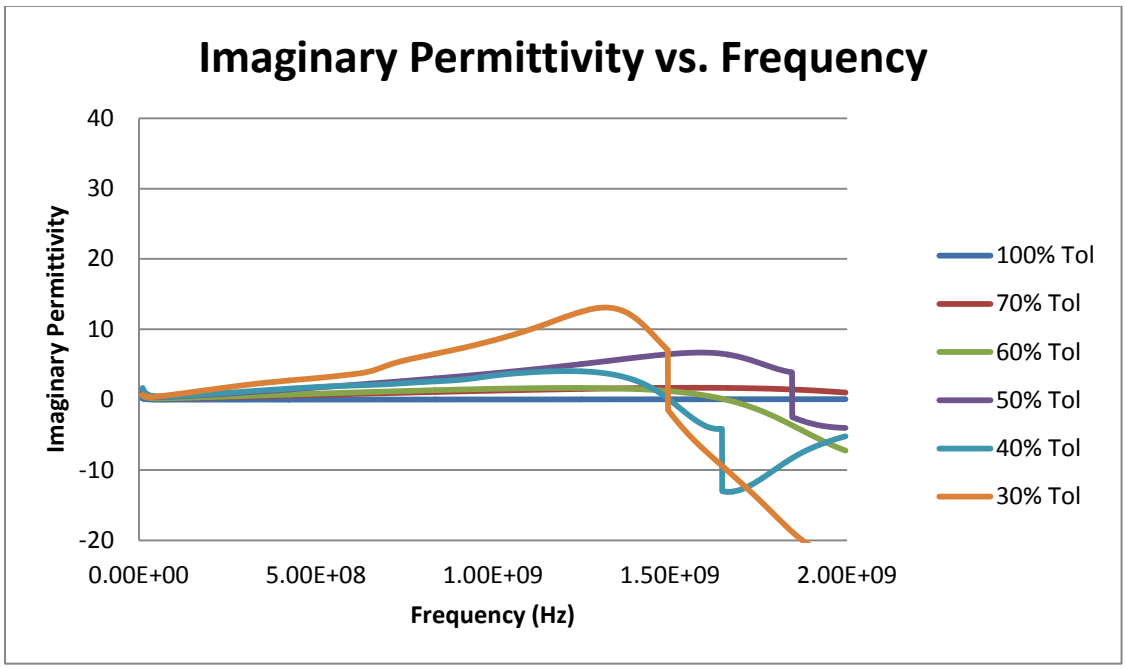

Figure 23. Imaginary Permittivity with AF455

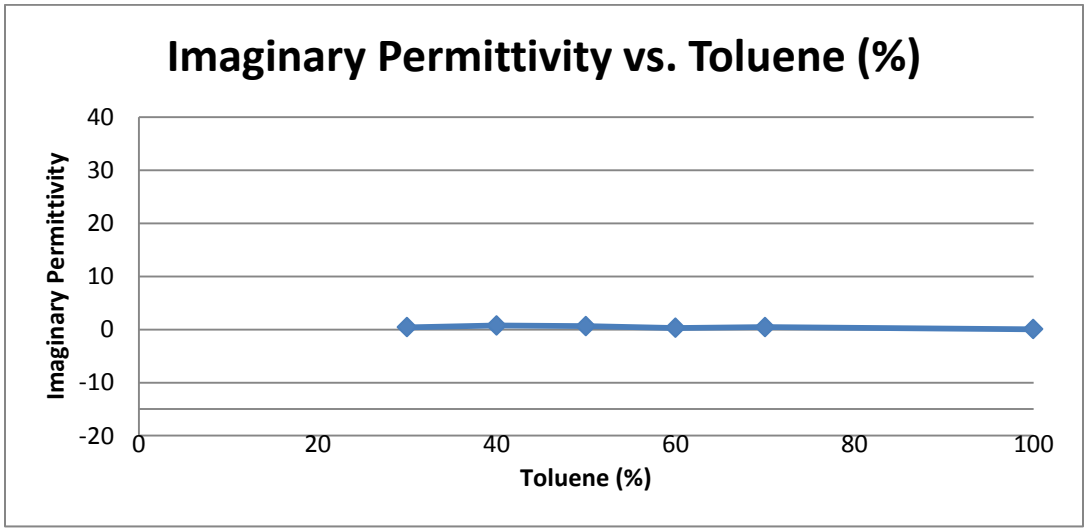

Figure 24. Imaginary with AF455 at 250 MHz

The values of imaginary permittivity with the addition of AF455 are also about zero, as expected. Figures 25 and 26 show the imaginary permittivity for the solvent blends with DNA-CTMA.

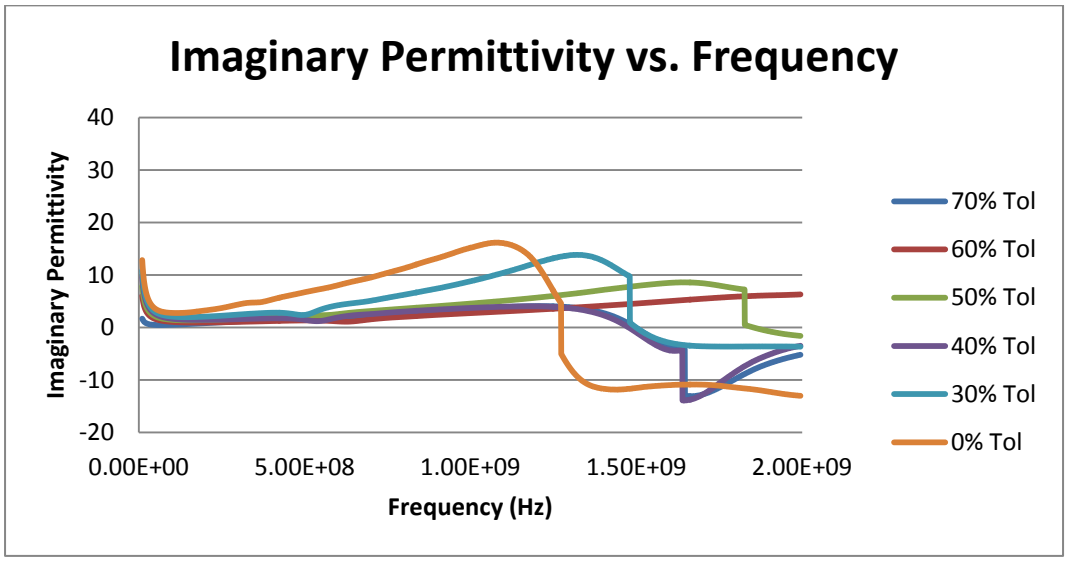

Figure 25. Imaginary Permittivity with DNA-CTMA

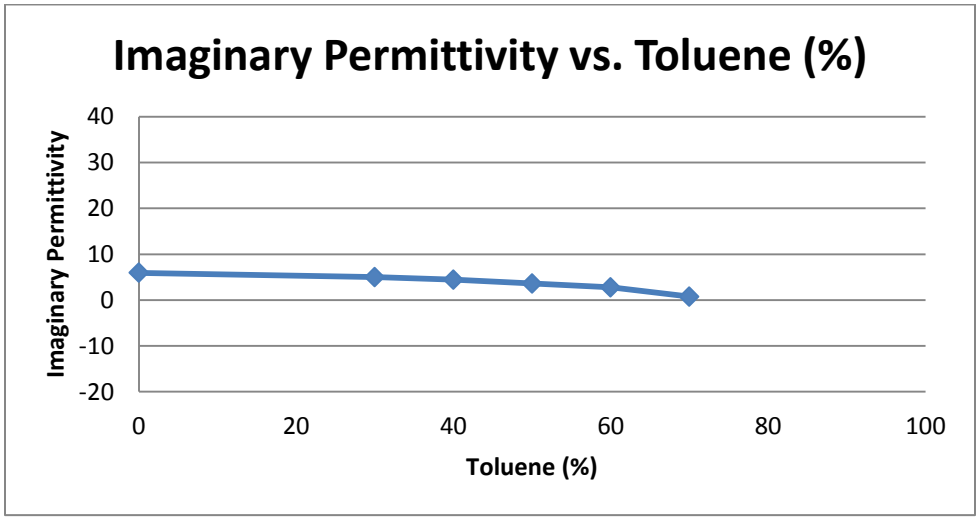

Figure 26. Imaginary Permittivity with DNA-CTMA at 250 MHz

The value of imaginary permittivity with DNA-CTMA is much higher than the solvent blends and the solvent blends plus AF455. This is expected since DNA-CTMA is a more complex structure. The permittivity decreases with increasing percent toluene. The decrease can be explained due to the conformation of the DNA-CTMA. The coil structure appears to be more lossy than a helix structure. Figures 27 and 28 have the results for all combined materials.

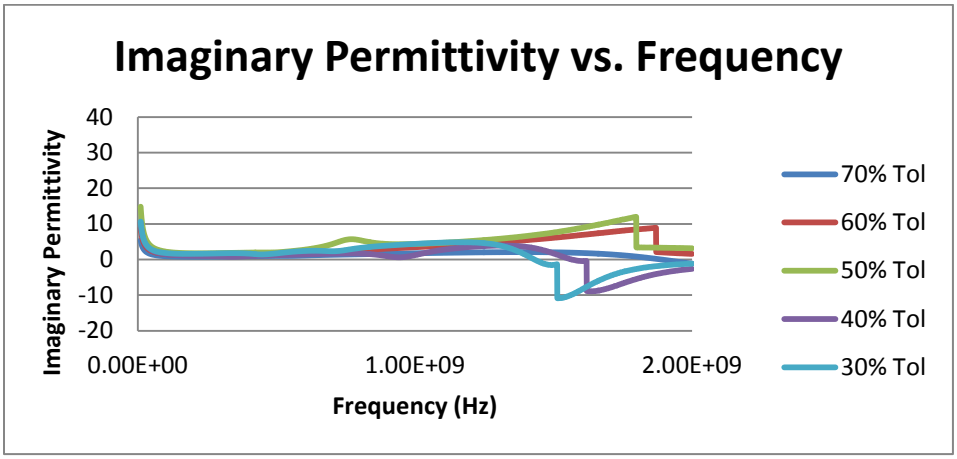

Figure 27. Imaginary Permittivity with AF455 and DNA-CTMA

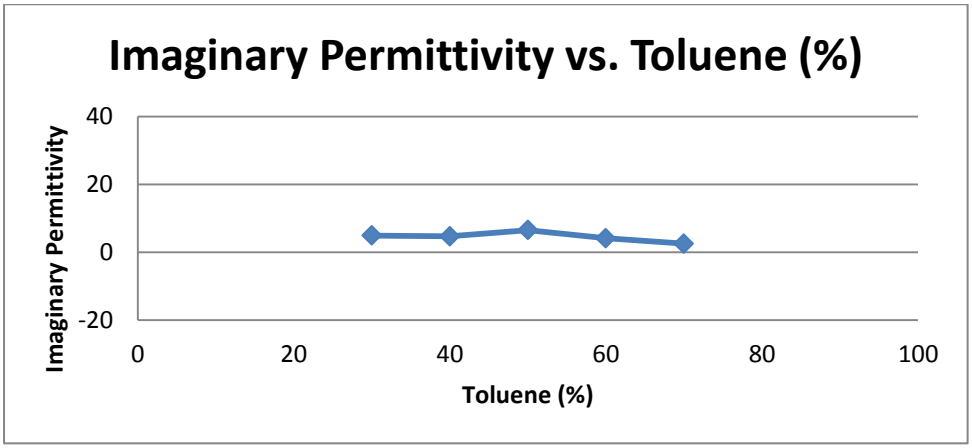

Figure 28. Imaginary Permittivity with AF455 and DNA-CTMA at 250 MHz

The value for the imaginary permittivity with both AF455 and DNA-CTMA is about 4.5. It is higher for the 50-50 blend and lower for the 70-30 blend. The way the AF455 binds with the DNA-CTMA could contribute to this effect as well as the conformation. Figure 29 shows all of the samples as a function of percent toluene.

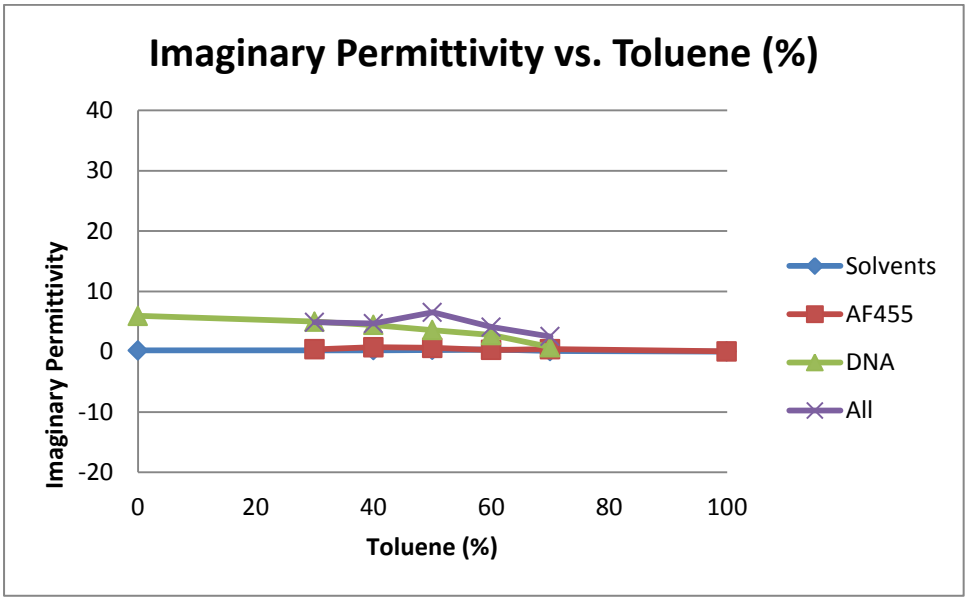

Figure 29. Imaginary Permittivity vs. Percent Toluene for 250 MHz

This graph shows the increase of imaginary permittivity for DNA-CTMA and all materials as compared to the solvents and AF455. Table 12 gives the values for 250 MHz.

Table 12. Imaginary Permittivity Values at 250 MHz

Percent Toluene	Imaginary Permittivity			
	Solvents	AF455	DNA-CTMA	All
100	0.028	0.055	-	-
70	0.099	0.43	0.73	2.51
60	0.36	0.28	2.76	4.08
50	0.29	0.62	3.58	6.52
40	0.23	0.73	4.42	4.67
30	-	0.40	5.00	4.89
0	0.20	-	5.93	-
Average	0.29	0.42	3.74	4.53

The electric loss tangent, Table 13, is trivial for the solvent blends and solvents plus AF455. However, it is an order of magnitude larger when the DNA-CTMA is included.

Table 13. Electric Loss Tangent for 250 MHz

Percent Toluene	Electric Loss Tangent			
	Solvents	AF455	DNA-CTMA	All
100	0.01	0.02	-	-
70	0.01	0.03	0.02	0.16
60	0.02	0.02	0.13	0.16
50	0.01	0.03	0.14	0.21
40	0.01	0.02	0.13	0.14
30	-	0.01	0.13	0.13
0	0.004	-	0.11	-
Average	0.01	0.02	0.11	0.16

4.1.4 Summary of Permittivity Results

The results of the real permittivity section indicate there is no interaction between the solvent blends. Table 10 lists the theoretical values of the real permittivity if the solvents behave as a pure mixture and the experimental data. The values are all within range.

When AF455 is added to the solvent blends, there is a slight decrease in overall permittivity. This could be the result of an interaction between the dipole moment of the "arms" of the AF455 molecule. This effect is very tiny, however.

Adding DNA-CTMA to the solvent blends does not affect the permittivity at all except for the 70-30 blend. The increase of permittivity in the 70-30 sample is indicative of a conformation change. The CD data suggests the conformation is a helix shape in this solvent blend.

When AF455 and DNA-CTMA is added into the solvent blends, there is an increase in the permittivity of the 50-50 and 60-40 blends. Previous work suggests binding between the AF455 and DNA-CTMA can cause this. Additionally, the conformation change in the 70-30 blend is not observed. The binding between the two could also cause this.

The imaginary permittivity for all samples is very low, as is expected. The real permittivity is fairly constant across the frequency range. The relationship between real permittivity and imaginary permittivity is a derivative over frequency, therefore, the expected values should be very low.

The imaginary permittivity increases when DNA-CTMA is added, indicating this is a lossy material. The imaginary permittivity increases for decreasing toluene percent. This is evidence of the conformation change also observed in the real permittivity. A coil structure is more lossy than a helix structure. When all materials are added, the imaginary permittivity is

lower for the 70-30 blend and higher for the 50-50 blend. This is due to the binding between AF455 and DNA-CTMA and the conformation change.

Though there are changes for some of the samples, the results are not dramatically different. The interesting properties of the TPA, AF455, are not evident in this range. The permittivity of the samples is not very different from the solvent blends themselves. The most interesting observation is the detection of a strong conformation change of the DNA-CTMA in the permittivity. The DNA-CTMA is more lossy than the samples without it, but this is expected since the molecule is very complex.

5.0 CONCLUSIONS

The real permittivity data gives the most information about the liquid blends. There is a slight reduction in AF455 when added to the solvent blends. This change could be the result of the dipole moment of the "arms" of the AF455 molecule reducing the overall field. When DNA-CTMA is added to the solvent blends, a strong conformation change is evident. The sharp increase in permittivity is due to the polarity of the DNA in a helix structure. This change was confirmed with CD measurements. When all materials are combined, there is an increase in permittivity for the 50-50 and 60-40 blends. Binding between the AF455 and DNA-CTMA increases the polarity of these samples. The imaginary permittivity is low for these materials indicating they are not very lossy. The blends with DNA-CTMA are higher, but this is expected since DNA-CTMA is a complex molecule.

The real permeability is consistent across all the samples, see Table 14. This indicates the material is isotropic and paramagnetic. The imaginary permeability is also consistent across all the samples, Figure 48. Table 16 displays the magnetic loss tangent. These materials are more lossy in the magnetic part than the electric part.

In this work, finding the conformation change of the DNA-CTMA with the permittivity is the most significant. There is also evidence of binding between the DNA-CTMA and AF455 in this frequency range. Future work can look into the details of the binding between the two materials. Additionally, work into the binding will help optimize the absorption of light for each of the solvent mixtures. Other interesting research measuring the relative permittivity and permeability values in the UV-Vis-NIR range. Developing a model for the optical properties and the effects of the various materials are of interest.

REFRENCES

(1) Taylor-Price II, Archie, "Absorbance of AF455 in Toluene: DMSO Solvent Blends," (Paper by a Thurgood Marshall Scholar under Dr. Angela Campbell at AFRL).

(2) Robinson, Paul, "Study Interaction of DNA-CTMA and AF455 in Different Solvent Mixtures Using Spectroscopic Methods," (2012 Presentation at AFRL under Dr. Angela Campbell).

(3) Sonmezogula, Savas, et al., "Optical and Dielectric Properties of Double Helix DNA Thin Films," *Materials Science and Engineering C*, Vol. 31, p. 1619, 2011.

(4) Heckman, Emily, et al., "Processing Techniques for Deoxyribonucleic Acid: Biopolymer for Photonics Applications," *Applied Physics Letters*, Vol. 87, p. 211115, 2005.

(5) Dr. Angela Campbell, personal communications

(6) Grote, James, et al., "Deoxyribonucleic Acid (DNA) Cladding Layers for Nonlinear Optic Polymer Based Electro-Optic Devices," *Organic Photonic Materials and Devices V*, Vol 4991, p. 621, 2003.

(7) Maarel, JRC, "Effect of Spatial Inhomogeneity in Dielectric Permittivity on DNA Double Layer Formation," *Biophysical Journal*, Vol. 76, p. 2673, 1999.

(8) Norwood, RA, et al., "Dielectric and Electrical Properties of Sol-Gel/DNA Blends," *Naobiosystems: Processing, Characterization, and Applications II*, Vol. 7403, p. 74030A-1, 2009.

(9) Goldberg, Jason, "Asexual Reproduction," Goldie's Room: On-Line, http://www.goldiesroom.org/Note%20Packets/14%20Mitosis%20and%20Asexual/00%20Mitosis--WHOLE.htm, (accessed 14 Nov 13).

(10) Yu, Zhou, "Optical Properties of Deoxyribonucleic Acid (DNA) and its Application in Distributed Feedback (DFB) Laser Device Fabrication," PhD Thesis, University of Cincinnati, 2006.

(11) Thirumaran, S. et al., "Acoustical Studies on Binary Liquid Mixtures of Some Aromatic Hydrocarbons with Dimethylsulfoxide (DMSO) at 303.15K," *Archives of Physics Research*, Vol. 2, p. 149, 2011.

(12) Campbell, Angela, Kozlowski, Gregory, Kleismit, Richard, Check, Michael, and Naik, Rajesh, "Microwave Characterization of DNA Biopolymer/Two Photon Absorber Thin Films Deposited by Matrix Assisted Pulsed Laser Evaporation," Unpublished Manuscript, 2013.

(13) Fox, Mark. Optical Properties of Solids, 2nd edition, New York: Oxford University Press, 2010.

(14) Dhanapala, Yasas, " Dielectric Constant Measurements Using Atomic Force Microscopy System," MS Thesis, Wright State University, 2012.

(15) Griffiths, David, Introduction to Electrodynamics, 3rd edition, Upper Saddle River: Prentice-Hall, Inc. 1999.

(16) He, Guang S. et al., "Multiphoton Absorbing Materials: Molecular Designs, Characterizations, and Applications," *Chemical Reviews*, Vol. 108, p. 1245, 2008.

(17) Rogers, Joy et al., "Understanding the One-Photon Photophysical Properties of a Two-Photon Absorbing Chromophore," *Journal of Physical Chemistry A*, Vol. 108, p. 5514, 2004.

(18) Sigma-Aldrich, "Sigma-Aldrich MSDS Search and Product Safety Center," http://www.sigmaaldrich.com/safety-center.html, (accessed 17 Oct 2013).

(19) Bellizzi, G, et al., "Broadband Spectroscopy of the Electromagnetic Properties of Aqueous Ferrofluids of Biomedical Applications," *Journal of Magnetism and Magnetic Materials*, Vol. 322, p. 3004, 2010.

(20) Fasman, Gerald D. ed, Circular Dichroism and the Conformational Analysis of Biomolecules, New York: Plenum Press, 2006.

(21) Issa, Hadil, Private Communications.

(22) Undre, P.B. et al., "Dielectric Relaxation in Ethylene Glycol-Dimethyl Sulfoxide Mixtures as a Function of Composition and Temperature," *Journal of the Korean Chemical Society*, Vol. 56, p. 41, 2012.

(23) Navarathne, Palamu ADS, "Conjugated Polymers and DNA for Photovoltaic and Photonic Applications," PhD Thesis, University of Connecticut, 2011.

LIST OF SYMBOLS, ABBREVIATIONS, AND ACRONYMS

Acronym	Description
AFRL	Air Force Research Laboratory
CD	Circular Dichroism
CTMA	Cetyltrimethyl ammonium
DMSO	Dimethyl sulfoxide
DOD	Department of Defense
MAPLE	Matrix assisted pulsed laser evaporation
OECL	Open ended coaxial line
RX	Materials & Manufacturing Directorate
SCCL	Short closed coaxial line
SOCHE	Southwestern Ohio Council for Higher Education
SOCL	Short open coaxial line
TPA	Two Photon Absorption
USAF	United States Air Force
WPAFB	Wright-Patterson Air Force Base